

# Read Static Noise Margin Fluctuation Induced by Various Random Discrete Dopants on 6T SRAM with Nanowire FET (NWFET) and Hybrid FinFET-NWFET Cells

Wen-Li Sung<sup>1-3</sup> and Yiming Li<sup>1-4,\*</sup>

<sup>1</sup>Parallel and Scientific Computing Laboratory, National Chiao Tung University, 1001 Ta-Hsueh Rd., Hsinchu 300, Taiwan

<sup>2</sup>Institute of Communications Engineering, National Chiao Tung University, 1001 Ta-Hsueh Rd., Hsinchu 300, Taiwan

<sup>3</sup>Department of Electrical and Computer Engineering, National Chiao Tung University, 1001 Ta-Hsueh Rd., Hsinchu 300, Taiwan

<sup>4</sup>Center for mmWave Smart Radar Systems and Technologies, National Chiao Tung University, Hsinchu 300, Taiwan

\*Tel: +886-3-5712121 ext. 52974; Fax: +886-3-5726639; Email: ymli@faculty.nctu.edu.tw

## Abstract

We for the first time report the variability of gate-all-around silicon nanowire MOSFET (NWFET) and 6T SRAM with NWFET and hybrid FinFET-NWFET cells induced by random discrete dopants (RDDs). Compared to all RDDs from channel and S/D extension, the normalized read static noise margin fluctuations ( $\sigma_{RSNM}$ ) with 6T NWFET-based cells can be suppressed ~54% without channel doping and penetration due to the reduction of fluctuation of saturation current ( $I_{sat}$ ). The access transistors possess the largest  $\sigma_{RSNM}$  than that of the driver and load transistors owing to the relatively larger variation of  $I_{sat}$  during the read operation. The  $\sigma_{RSNM}$  with 6T hybrid FinFET-NWFET cells ( $RSNM = 194$  mV) was smaller than that of 6T NWFET-based cells as compared to 6T NWFET-based cells ( $RSNM = 125$  mV) for all RDDs due to increasing read static noise margin.

## 1. Introduction

A 6T SRAM with hybrid TFET-FinFET cells was proposed to increase read static noise margin (RSNM) and decrease leakage power due to the considerations of low power consumption, high performance and low area of chip [1]. However, the reports showed that 6T SRAM with FinFET cells suffered large variations from random dopant fluctuation (RDF), work function fluctuation (WKF) and process variation effect (PVE), especially RDF [2-3]. Gate-all-around (GAA) nanowire MOSFET (NWFET) is one of attractive devices for sub-5-nm technology nodes, but various fluctuations also have yield problems [4-5]. Characteristic fluctuations induced by various RDDs of GAA Si NWFETs have been studied [6]. And, the FinFET's process is compatible with GAA NWFET's process with relatively low complexity [7]. Hence, it is important to investigate the influence of RDDs on the variation of RSNM with NWFET and hybrid FinFET-NWFET cells, respectively.

In this study, we for the first time explore the fluctuated GAA NWFET devices, 6T SRAM with NWFET and hybrid FinFET-NWFET cells caused by various RDDs. We consider the cases with all RDDs from channel and S/D extension including their penetration (denoted as  $RDDs_{ch\_Sext\_Dext\_pe}$ ), without penetration from S/D extensions into channel (denoted as  $RDDs_{ch\_Sext\_Dext}$ ), without channel doping (denoted as  $RDDs_{Sext\_Dext\_pe}$ ), and without channel doping and penetration from S/D extensions into the channel (denoted as  $RDDs_{Sext\_Dext}$ ).

## 2. Coupled Device-Circuit Simulation Methodology

The simulation is performed intensively by solving a 3D quantum-mechanically corrected transport model that has been validated through the nonequilibrium Green's function (NEGF) results by tuning the electron effective mass [4,6]. To provide the best accuracy of simulation, not shown here, we calibrate the simulation results of the 3D quantum-mechanically corrected transport model with measured Si data by fitting the parameters of mobility model [4]. The concentration and distribution for the four types of RDDs that are statistically generated by Monte Carlo method for both N-/P-type devices [6,8]. The 6T SRAM with NWFET and hybrid

FinFET-NWFET cells are then considered to estimate the RSNM fluctuations, as shows in Fig. 1. Finally, we normalize the fluctuations of the characteristic parameters of N-/P-type devices and  $\sigma_{RSNM}$  of SRAM circuit by  $(6\sigma/\mu) \times 100\%$ , where  $\sigma$  is the standard deviation of the variation, and  $\mu$  is the average of the characteristic parameters.

## 3. Results and Discussion

Fig. 2 shows the fluctuated  $I_D$ - $V_G$  curves induced by various sources of RDDs, respectively. The standard deviation and the average of the characteristic parameters of N-/P-type devices are extracted from Fig. 2. Table I summarizes the variation of DC characteristics. We find that the variation of saturation current ( $I_{sat}$ ) can be reduced without channel doping and penetration due to the reduction of the variation of threshold voltage ( $V_{th}$ ). However, the reduction of the  $g_{m,max}$  variations was not as pronounced. The RSNM is extracted from butterfly characteristic fluctuation curves of 6T SRAM with NWFET cells, as shown in Fig. 3, where the dashed lines are intrinsic-parameter-fluctuated curves, and the solid line stands for the nominal curve. Fig. 4 shows the variation of 6T SRAM with NWFET cells by considering the RDDs in different transistor pairs. The  $\sigma_{RSNM}$  can be reduced from 12.6 to 5.8% without channel doping and penetration and the  $\sigma_{RSNM}$  with penetration is smaller than that with channel doping. The inset shows the access transistors have the largest  $\sigma_{RSNM}$  during read operation. According to the proportional Eq. (1) between DC characteristics and RSNM [3,9],

$$RSNM \propto \sqrt{1 - \frac{I_{nx}}{g_{m,P-MOS}}} - \frac{I_{ax}}{g_{m,N-MOS}}, \quad (1)$$

where the  $I_{nx}$  and  $I_{ax}$  are the saturation drain currents of the driver and access transistors. We find that the variation of the saturation drain current of access transistor dominates the variation of RSNM at the similar  $g_{m,max}$  variations. The fluctuation of access transistors dominates the RSNM fluctuation for all cases of RDDs. Fig. 5(a) shows that RSNM with hybrid FinFET-NWFET cells can be enlarged and then, the  $\sigma_{RSNM}$  with 6T hybrid FinFET-NWFET cells can be improved up to 58% (i.e.,  $(12.6-5.3)/12.6 \times 100\%$ ) as compared to NWFET cells, as shown in Fig. 5(b).

## 3. Conclusions

In summary, we have found that the fluctuation of RSNM is mainly governed by doped channel and the access transistors. The magnitude of  $\sigma_{RSNM}$  of the tested 6T SRAM with hybrid FinFET-NWFET cells can be suppressed effectively.

## Acknowledgment

This work was supported in part by the Ministry of Science and Technology (MOST), Taiwan, under grants MOST 106-2221-E-009-149, MOST 106-2622-8-009-013-TM, and MOST 107-3017-F-009-001, a grant from Taiwan Semiconductor Manufacturing Company in 2016-2017, and the "Center for mmWave Smart Radar Systems and Technologies" under the Featured Areas Research Center Program within the framework of the Higher Education Sprout Project by the Ministry of Education (MOE) in Taiwan.

## References

- [1] H. Afzali-Kusha, A. Shafaei, and M. Pedram, in: *Proc. IEEE ISQED*, pp. 280-285, 2018.
- [2] Y. Li, C.-Y. Chen, and Y.-Y. Cheng, *Int. J. Nanotech.*, pp. 1029-1038, 2014.
- [3] Y. Li, H.-W. Cheng, and M.-H. Han, *IEEE T. SM*, pp. 509-516, 2010.
- [4] Y. Li et al., in *IEDM Tech. Dig.*, pp. 887-890, 2015.
- [5] N. Mori et al., in *IEDM Tech. Dig.*, pp. 116-119, 2013.
- [6] W.-L. Sung and Y. Li, *IEEE T. ED*, pp. 2638-2646, 2018.
- [7] H. Mertens et al., in *IEDM Tech. Dig.*, pp. 524-527, 2016.
- [8] W.-L. Sung, P.-J. Chao and Y. Li, in *IEEE SISPAD*, pp. 61-64, 2017.
- [9] A. J. Bhavnagarwala et al., *IEEE J. SSC*, vol. 36, pp. 658-665, 2001.

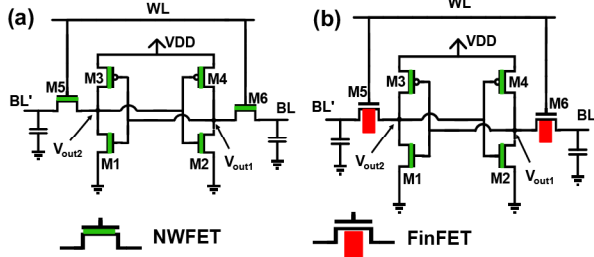


Fig. 1. 6T SRAM circuit with (a) NWFET cells. (b) Hybrid NWFET-FinFET cells, where M1 and M2 are driver transistors, M3 and M4 are load transistors, and M5 and M6 are the access transistors. The configuration of structure and device parameters mainly follow our recent investigation on NWFET and FinFET devices in [2,6].

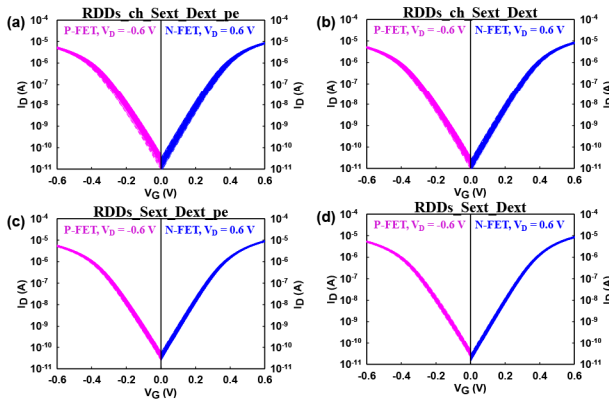


Fig. 2. The  $I_D$ - $V_G$  characteristic fluctuation curves of the studied device induced by various sources of RDDs. (a) RDDs\_ch\_Sext\_Dext\_pe, (b) RDDs\_ch\_Sext\_Dext, (c) RDDs\_Sext\_Dext\_pe, and (d) RDDs\_Sext\_Dext.

Table I. List of the variation percentages of the parameters of electrical characteristics induced by the various types of RDDs. The variation percentage is calculated by  $(6\sigma/\text{Mean value}) \times 100\%$ , where  $\sigma$  is the standard derivation of the parameters, and the mean value is the average of the parameters.

Type	Parameters	$V_{th}$	$g_{m,max}$	$I_{sat}$
N-FET	RDDs_ch_Sext_Dext_pe	19.6	22.0	22.9
	RDDs_ch_Sext_Dext	17.0	21.8	22.3
	RDDs_Sext_Dext_pe	12.2	20.9	18.1
	RDDs_Sext_Dext	8.9	21.1	19.5
p-FET	RDDs_ch_Sext_Dext_pe	21.6	14.5	26.4
	RDDs_ch_Sext_Dext	19.1	14.3	25.4
	RDDs_Sext_Dext_pe	14.0	14.2	20.1
	RDDs_Sext_Dext	11.0	14.3	19.2

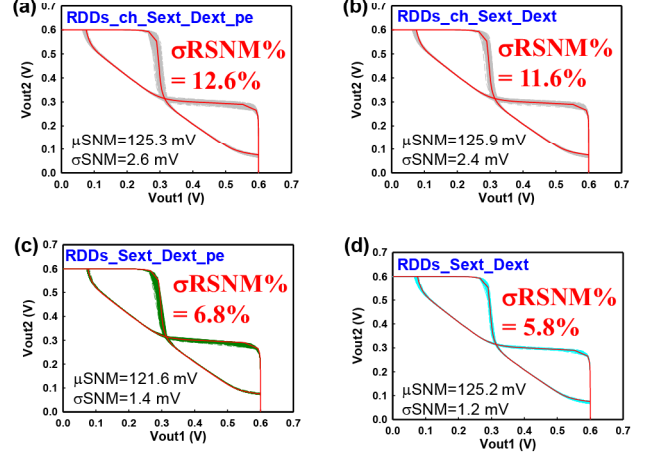


Fig. 3. The curves of butterfly characteristic fluctuation of the 6T SRAM with NWFET cells induced by various sources of RDDs. (a) RDDs\_ch\_Sext\_Dext\_pe, (b) RDDs\_ch\_Sext\_Dext, (c) RDDs\_Sext\_Dext\_pe, and (d) RDDs\_Sext\_Dext, respectively.

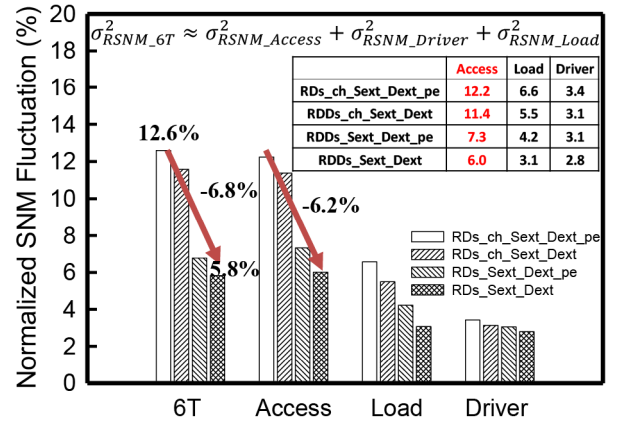


Fig. 4. The influence of different transistor pairs on total RSNM fluctuation of the explored 6T SRAM with NWFET cells induced by various sources of RDDs. Reduction ratio =  $(12.6 - 5.8)/12.6 \times 100\% = 54\%$ .

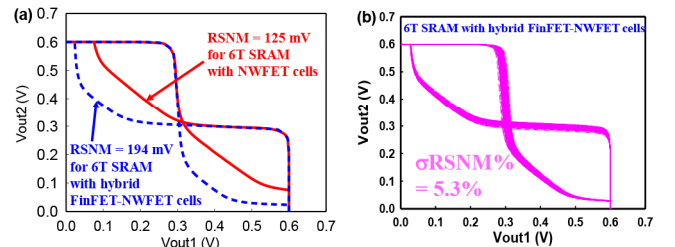


Fig. 5. (a) The nominal butterfly curves of the explored 6T SRAM with NWFET cells ( $RSNM = 125$  mV) and with hybrid NWFET-FinFET cells ( $RSNM = 194$  mV). More than 35% increase on RSNM. (b) The RDF-fluctuated butterfly curves of the explored 6T SRAM with hybrid NWFET-FinFET cells. Reduction of  $\sigma_{RSNM}$  has been achieved from 12.6%, as pointed out in Fig. 3(a), to 5.3%.